Local defect-free elastic strain relaxation of $Si_{1-x}Ge_x$ embedded into SiO_2

Elie Assaf [1], Isabelle Berbezier[1*], Mohammed Bouabdellaoui[1], Marco Abbarchi[1], Antoine Ronda[1], Damien Valenducq[2], Fabien Deprat[2], Olivier Gourhant[2], Andreas Campos[3], Luc Favre[1]

[1]*CNRS, IM2NP, Aix-Marseille University, Faculté des Sciences de Saint-Jérôme, case 142, 13397 Marseille, France*

[2]*Digital Front End Manufacturing & Technology STMicroelectronics Crolles, France*

[3]*CP2M, Service 221, Campus Scientifique de Saint Jérôme, 13397 Marseille cedex 20*

Abstract

We show that a newly developed high temperature, ultra-low rate oxidation process can produce fully strained, defect-free and perfectly flat Silicon Germanium ($Si_{1-x}Ge_x$) On Insulator films when $x \leq 0.33$. For larger Ge concentrations ($x = 0.5$), we evidence a new mechanism of elastic strain relaxation taking place through the undulation of the $Si_{1-x}Ge_x$ layer without nucleation of dislocations. In these experimental conditions (ultra-low rate oxidation at 1000°C), strain relaxation proceeds through the slow diffusion and motion of matter at the $Si_{1-x}Ge_x/SiO_2$ interface and not through dislocation nucleation. The mechanism results in the morphological evolution and local swelling of the SiGe embedded layer, facilitated by the viscous flow of SiO_2. At these temperatures, the $Si_{1-x}Ge_x$ film expands in the viscous SiO_2 to minimize the strain energy. Geometric Phase Analysis of High Resolution Transmission Electron Microscopy cross-section images confirms that the lateral expansion leads to the relaxation of the strain accumulated during condensation of Ge. We suggest that this phenomenon could be at the origin of the buckling mechanism already reported in the literature.This study demonstrates that SiO_2 can serve as an efficient compliant substrate for strain engineering of defect-free Ge rich $Si_{1-x}Ge_x$ thin films. This new generic relaxation process based on SiO_2 matrix viscoelasticity could be applied to many other systems beyond $Si_{1-x}Ge_x$ films. The high-quality defect-free Ge rich SGOI films fabricated here can act as good template for the heterogeneous integration of various 2D or 3D materials on Si substrate.

Introduction

Germanium (Ge) and silicon-germanium ($Si_{1-x}Ge_x$) thin film research is a subject of considerable interest in microelectronics since the 90's, due to the high mobility of electrons and holes in thin films based on Ge compared to silicon (Si) [1-6]. In addition, the increase of the carriers mobility (both electrons and holes) by strain engineering which modifies the band structure [7-9], has been reported to significantly improve the performance of microelectronics devices [10]. Ge-based thin films were then rapidly, considered as indispensable for the production of high-performance metal-oxide-semiconductor field-effect transistors (MOSFETs) for microelectronics technology [11-16] and for low loss waveguides for Mid-infrared Silicon

photonics [17-19]. Research on $Si_{1-x}Ge_x$ has reappeared as a topic of interest with the development of Fully Depleted Silicon On Insulator (FD-SOI) technology [20] where compressively strained $Si_{1-x}Ge_x$ channels (or tensilely strained Si channels on relaxed $Si_{1-x}Ge_x$) have been engineered to increase the level of stress to benefit pMOS and nMOS transistors [13, 21-23]. The ability to fabricate fully strained SOI and $Si_{1-x}Ge_x$ on insulator (SGOI) layers offers various advantages for producing mixed substrates in which the n-channels consist of a thin SOI layer, while the p-channels consist of thin SGOI layer [24,25]. More precisely, for advanced CMOS technologies, one promising way is to cointegrate a Si channel tensilely strained in nMOS transistors and a compressively strained $Si_{1-x}Ge_x$ channel for pMOS transistors. This cointegration allows simultaneous improvement of electron and hole mobility compared to unstrained materials. The strain integration along the specific <110> directions on (100)Si provides the best gain in mobility for the two transistors [26]. Moreover, Ge rich $Si_{1-x}Ge_x$ films that can be integrated in waveguide/device combination fulfill both transparency of the Si waveguide and strong light-matter interaction in a large wavelength regime. They have been presented recently as booster of the Si photonics [27]. SGOI layer is obtained by thermal oxidation of a $Si_{1-x}Ge_x$ /SOI heteroepitaxy system [28,29] resulting into a top silicon oxide layer (SiO_2) and a Ge-rich layer underneath [23,30]. During this process, called Ge condensation, Si oxidizes preferentially while Ge atoms are pushed at the SiO_2/ $Si_{1-x}Ge_x$ interface resulting in a thin Ge-rich $Si_{1-x}Ge_x$ layer at this interface. After condensation, the $Si_{1-x}Ge_x$ / Si layers are embedded between the two SiO_2 barriers, since the growing SiO_2 layer on top and the buried oxide (BOX) layer act as barriers against Si and Ge diffusion [31]. Different processes have been developed to produce homogeneous $Si_{1-x}Ge_x$ layer starting from $Si_{1-x}Ge_x$ /SOI heterojunctions. They commonly imply first an oxidation which produces Ge pile-up at the oxidation front and second an annealing to homogenize the resulting $Si_{1-x}Ge_x$ layer [32]. The layer obtained is commonly under biaxial compressive strain [33,34]. Sugiyama et al. [35] have found that at high-temperature oxidation (1200°C), a flat Ge profile SGOI layer with low density of dislocations can be obtained, due to the diffusion of Ge which overcomes the accumulation of Ge atoms at the interface. They claim that for a "Separation by Implantation of Oxygen" (SIMOX) SOI, a high oxidation temperature promotes a fully relaxed SGOI layer with high Ge content (28%) and without dislocation. Moreover, Tezuka et al. [36] show that for an oxidation temperature of 1050°C, the Ge profiles along the SGOI layer are quite uniform and the layers are almost completely relaxed. However, the process does not remove the threading dislocations in the SGOI layers and it can be applied only to very thin layers (the effect of the SIMOX process for the fabrication of SOI is not addressed in this work). Furthermore, Anthony et al. [37] have shown that for a mixed process involving both Ge implantation and condensation techniques and based on Ge-implanted SOI, the $Si_{1-x}Ge_x$ layer is relatively uniform and defect free, with a significant compressive strain that evolves with temperature. They report a significant compressive strain of about 1% at 900°C while at 1000°C, this compressive strain is reduced to 0.7% due to the intermixing between the Si with the $Si_{1-x}Ge_x$ layer and the $Si_{1-x}Ge_x$ layer is completely relaxed at 1080 °C. A recently developed process based on condensation/annealing steps has created tensilely strained Si layers epitaxially grown on relaxed SGOI with −0.85% tensile strain in the out-of-plane direction for multifinger 2.5 V n-type MOSFET on SOI for RF-switch applications [38]. In parallel, it was reported that during high temperature treatment, the SiO_2 film becomes viscous and the strained thin film on this viscous oxide is morphologically unstable. In this case, the relaxation of the film can occur due to the viscous flow of the $Si_{1-x}Ge_x$ film in the underlying oxide layer [39-45]. In these conditions, the relaxation mechanism to relieve stress results from the buckling of

the film. Relaxation of strained $Si_{1-x}Ge_x$ films by buckling on viscous oxide has been observed during long-time annealing at high temperatures [39-45].

In this work, we show that a newly developed oxidation process of Silicon Germanium on Silicon On Insulator (SGOI) that consists of high temperature ultra-low rate oxidation can produce Ge rich $Si_{1-x}Ge_x$ layers, totally free of dislocation. Depending on the Ge concentration in the Ge rich layer obtained after oxidation, the SGOI films are either fully strained or partially and locally relaxed. . In a first series of experiments we determine the optimalexperimental parameters that are used in the rest of the study, for the fabrication of continuous dislocation-free $Si_{1-x}Ge_x$ layer. The central part of the study is dedicated to the investigation of strain in the $Si_{1-x}Ge_x$ films after the ultra-low rate oxidation. The samples are characterized by SEM, AFM, Raman spectroscopy and TEM cross-section observations. The results show that when $x \leq 0.33$ after oxidation, the film remains fully strained and flat, while for x=0.5, undulations and swelling of the $Si_{1-x}Ge_x$ film accompanied by the correlated redistribution of matter (both $Si_{1-x}Ge_x$ and SiO_2) are observed locally. In this case, the GPA results demonstrate that these local protrusions of the $Si_{1-x}Ge_x$ film inside SiO_2 are systematically accompanied by a strong elastic relaxation of the film in the undulated areas, while the overal layer is still fully strained. We suggest that this phenomenon represents the first stage of elastic relaxation possibly leading to the buckling of the film in a subsequent relaxation step. The results show that the optimized oxidation process developed here could provide Ge rich $Si_{1-x}Ge_x$ layers totally free of extended defects, either fully strained with homogeneous thickness for $x \leq 0.33$ or locally elastically relaxed with small thickness inhomogeneities and small undulations for $x = 0.5$.

Experiments.

In this work, we use 300mm SOI wafers with Si nominal thickness of 11nm on 20nm buried oxide (BOX). The substrates are first thinned by thermal oxidation at 860°C followed by HF etching in order to get SOI thickness about 8nm. Prior to epitaxy, in-situ cleaning by Siconi is performed to ensure a SOI surface without SiO_2 residual. $Si_{1-x}Ge_x$ epitaxial layers were grown at 630°C, 10 Torr on the top of SOI with the system H_2/HCl/DCS (Dichlorosilane SiH_2Cl_2)/GeH_4 by low pressure chemical vapor deposition (LPCVD) tool. The investigated structures were fabricated at STMicroelectronics under standard conditions in a state-of-the-art 300mm technology semiconductor facility using SOI wafer. After epitaxy, dry furnace oxidation is performed between 750 and 1000°C. Those temperatures allow the fabrication of SGOI substrates with a large Ge concentration range, as they are lower than the $Si_{1-x}Ge_x$ melting temperature during Ge enrichment. A newly developed process of oxidation at very low oxygen partial pressure [46] was used. The very low oxygen partial pressure is obtained by dilution in nitrogen at 690Torr. A N_2/O_2 flux ratio of 30 is fixed during oxidation at the constant temperature. A few nm thermal oxide is grown during the heating ramp (even with the minimal flux of oxygen used). This layer further passivates the SGOI preventing its dewetting during oxidation at the constant temperature.

The effect of the oxidation conditions (temperature and time) on the morphological and structural evolution of the samples, is assessed by scanning electron microscopy (SEM) and atomic force microscopy (AFM) observations to bring out extended defects. Extended defects include both dislocation (dislocation loops, misfit dislocations and threading dislocations), stacking faults (commonly induced by impurities or inappropriate growth conditions) and pits

(induced by contaminants). We commonly look for cross-hatch patterns which result from the presence of threading and misfit dislocations. Micro Raman spectroscopy was performed systematically to check the structural quality and the strain of the epitaxial layer. Transmission electron microscopy (TEM) observations were performed on cross-section samples prepared using a FEI Helios 600 Dual Beam Ga^+ focused ion beam (FIB). High-resolution transmission electron microscopy (HR-TEM) observations were performed using a FEI Titan 80-300 Cs corrected microscope, operated at 200 keV. Geometric Phase Analyses (GPA) were performed on HR-TEM images, using Digital micrograph software. They give a local quantitative determination of the strain in the $Si_{1-x}Ge_x$ layers.

Results and discussion

The oxidation/condensation mechanism has been already explained in detail elsewhere [47, 48]. At low temperatures (<850°C), the selective oxidation of Si atoms produces a Ge rich layer (GRL) with a Ge content of 50%. This concentration remains constant to 50% throughout the condensation process until the complete consumption of all the SOI layer. This 50% concentration is obtained whatever the initial Ge content and the strain level of the $Si_{1-x}Ge_x$ nominal layer are (the same 50% concentration was found for initial Ge fraction varying from 10 to 30% and for strained and relaxed systems) [48]. When all the silicon is oxidized, the composition of the GRL increases up to pure Ge. During the condensation two main issues should be prevented: the nucleation of misfit dislocations and the solid state dewetting. Both dewetting and nucleation of dislocations are promoted by an increase of the Ge content which increases both the epitaxial strain and the diffusion at the SiO_2/ $Si_{1-x}Ge_x$ interface (at the origin of dewetting) [49-51]. Thereby, to determine the condensation conditions to get $Si_{1-x}Ge_x$ layers free of defect and homogeneous in thickness and composition, we first checked the onset of these mechanisms for different oxidation temperatures and times.

The optimal parameters for oxidation/annealing of $Si_{0.7}Ge_{0.3}$/SOI sample were determined in a first series of samples. The starting system consists of 26nm thick $Si_{0.7}Ge_{0.3}$ on SOI, which is then oxidized at low temperature (750°C) and annealed at higher temperature to homogenize the Ge composition (60min at ~900°C). Figure 1a gives the parameters of the starting system and the evolution expected after 90min and 210min oxidation followed by annealing (Figures 1b and 1c). The SEM images of the samples after oxidation and annealing are given in Figure 1d and 1e. They both evidence the presence of cross-hatch patterns representative of threading dislocations associated to misfit dislocations.

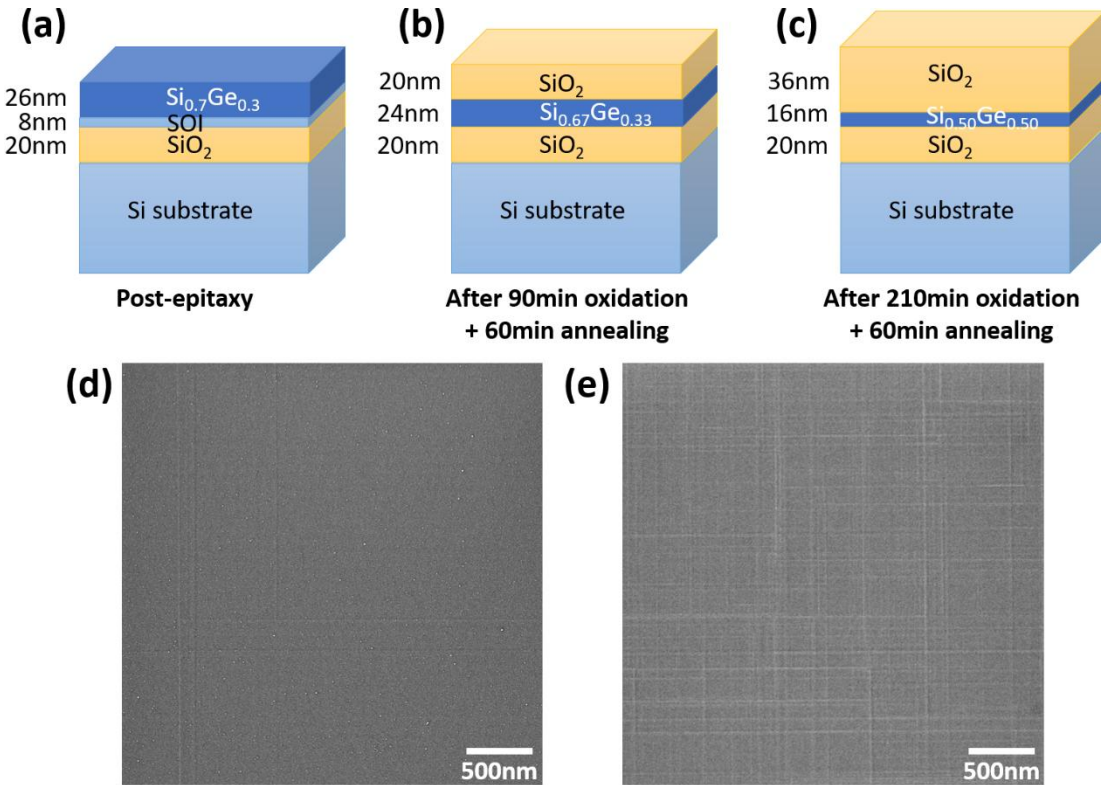

Figure 1: Schemas of the system (a) before and (b) and (c) after 90min and 210min oxidation at 750°C respectively. The two samples have been annealed (60min at 900°C) to homogenize the Ge composition. (d) and (e): SEM plane view of samples (b) and (c), respectively. Threading dislocations nets are visible on both surfaces.

As one might expect, the density of dislocations increases with the oxidation time (resulting from an increase of the Ge concentration from 33 to about 50%). Experiments with only oxidation (and no annealing) of similar $Si_{0.7}Ge_{0.3}$/SOI samples were carried out in the same experimental conditions. They evidenced an identical density of dislocations, highlighting the oxidation step (condensation of Ge) as the origin of the nucleation of dislocations. All these samples with dislocations are of course unsuitable for device applications. New experiments were then carried out with a lower thickness (20nm instead of 26nm) of $Si_{0.7}Ge_{0.3}$/SOI sample. After oxidation at 750°C for 210min and homogenization treatment at 900°C for 60min (similar conditions to those used for the previous experiments with 26nm $Si_{0.7}Ge_{0.3}$/SOI) , the SEM images evidenced the absence of dislocations (not shown here). However, TEM cross-section observations highlight an inhomogeneous distribution of the Ge throughout the layer well evidenced by an increasing absorption contrast of electrons from bottom to top in the SiGe layer (Figure 2a). Note that this inhomogeneity was also observed for the 26nm sample. To better homogenize this composition, an increase of the oxidation temperature (to 1000°C) was tested. It induces solid state dewetting even during the heating ramp of the process, as revealed on Figure 2b. It can be concluded from this series of experiments that for an initial $Si_{0.7}Ge_{0.3}$/SOI layer, it was not possible to get flat layer free of dislocation and with high Ge concentration. Either the composition is inhomogeneous (low temperature annealing), or the film dewets (higher annealing temperature, low initial thickness) or it is dislocated (higher initial thickness).

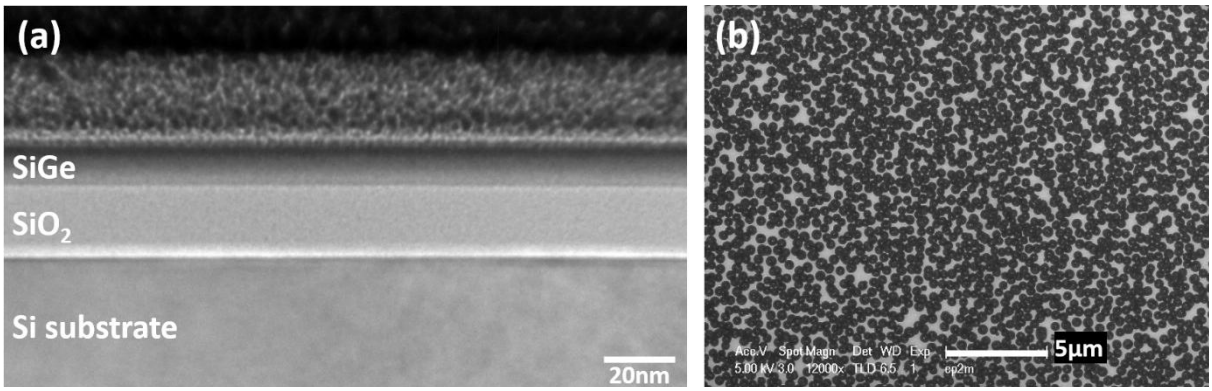

Figure 2: (a) TEM image of 20nm $Si_{0.7}Ge_{0.3}$ after oxidation and annealing; (b) SEM image of the dewetting process during the heating ramp of the sample.

These first results provide useful information on the optimal conditions to apply for the condensation process: the initial $Si_{0.7}Ge_{0.3}$ thickness should be ≤ 20nm (in order to decrease dislocation density); the annealing temperature should be larger than 750°C and the duration should be extended above 210 min (in order to homogenize the composition). A recently developed process (with a single step including low-rate oxidation and annealing) fulfils these requirements. In these conditions, an oxidation temperature around 1000°C was chosen. To prevent solid state dewetting of the $Si_{0.7}Ge_{0.3}$ layer during the sample heating, a very thin (2nm) chemical SiO_2, was grown by a HF-SC1 standard clean performed after epitaxy, before the oxidation step [46]. After the SiO_2 capping, the recently developed process based on dry thermal oxidation at 1000°C with ultra-small oxygen flux is carried out, for various oxidation times, allowing the fabrication of SGOI substrates with different concentrations of Ge.

In the rest of the study, we focus on the comparison of three samples: the initial sample which is composed of a 2nm SiO_2 chemical oxide on top of 15nm thick $Si_{0.7}Ge_{0.3}$ layer in epitaxy on SOI (Sample A); the two samples obtained after 120min and 300min oxidation (called Samples B and C respectively). The two latter samples are composed of $Si_{1-x}Ge_x$ layers (with ~14nm $Si_{0.67}Ge_{0.33}$ layer and ~9nm $Si_{0.50}Ge_{0.50}$ layer for samples B and C respectively) embedded between two SiO_2 layers. The newly developed condensation process is performed at very low oxygen partial pressure which produces an extremely slow oxidation rate, allowing both oxidation and annealing to be carried out in a single step [46]. A schematic representation of the three structures is given in Figure 3.

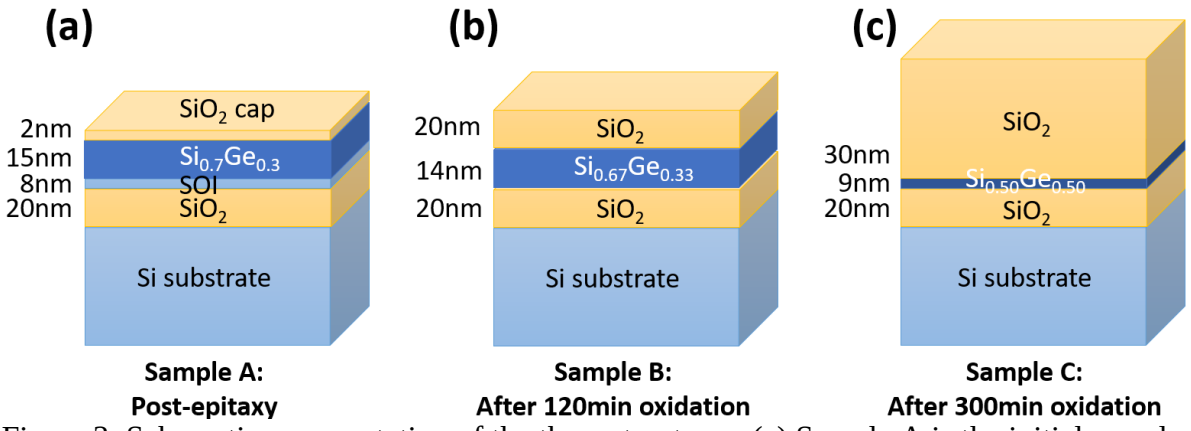

Figure 3: Schematic representation of the three structures: (a) Sample A is the initial sample composed of a 15nm thick $Si_{0.7}Ge_{0.3}$ layer on a 8 nm thick Si layer itself on the top of a

20nm thick SiO_2 (BOX). Samples B and C correspond to sample A after 120min and 300min oxidation respectively. (b) Sample B consists of a 14nm thick $Si_{0.67}Ge_{0.33}$ layer capped with a 20nm thick SiO_2 layer; (c) Sample C consists of a 9nm thick $Si_{0.5}Ge_{0.5}$ layer capped with a 30nm thick SiO_2 layer.

Before surface observations, the SiO_2 top layer of samples B and C were removed using HF etching. SEM images did not evidence any dislocation even on large scale and only the instrumental noise is visible. AFM images of samples B and C were then recorded to focus on the surface roughness (Figure 4). The surfaces of the two samples are continuous and flat (with RMS values around 0.15nm, in the range of the AFM signal noise in air) without visible features or extended defects, demonstrating the absence of dewetting and of nucleation of dislocations. The films are then expected to be fully strained [52].

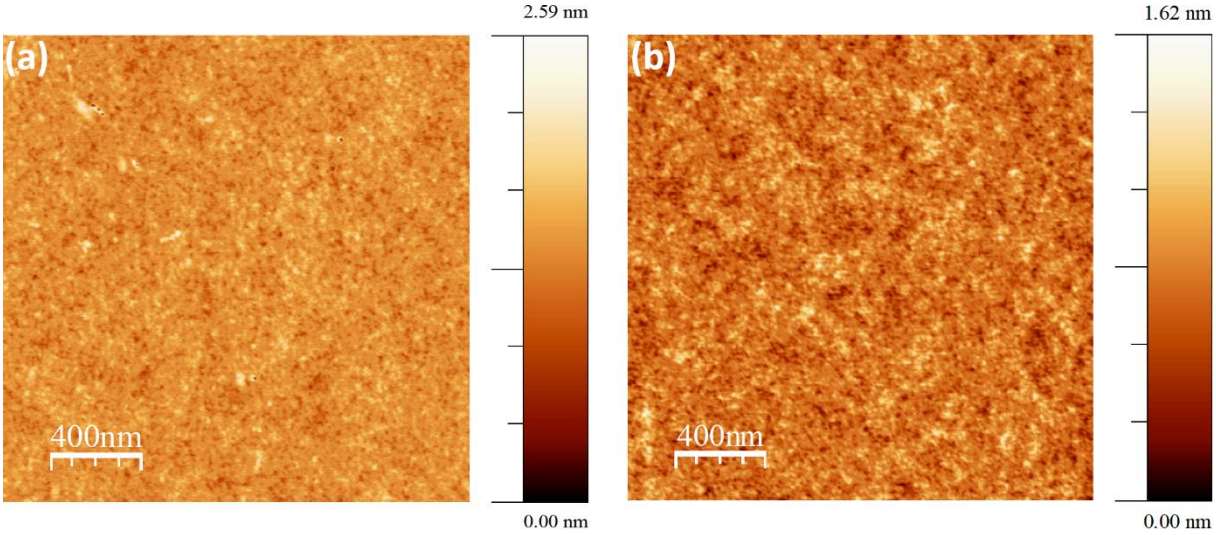

Figure 4: AFM images in air of (a) sample B (120min oxidation) and (b) sample C (300min oxidation) respectively.

To get quantitative information on the strain, micro Raman spectroscopy was carried out on the three samples. Figure 5 shows the evolution of the Raman vibration modes, with the oxidation time. The spectra are characterized by three optical vibration modes in addition to the Si substrate peak (~520cm^{-1}): Ge-Ge (~300cm^{-1}), Si-Ge (~420cm^{-1}) and Si-Si (~500cm^{-1}) modes, whose intensities are proportional to the p_{Si-Si}, p_{Si-Ge} and p_{Ge-Ge} probabilities. The frequencies and line widths of these three modes (Si-Si, Si-Ge and Ge-Ge) vary with Ge concentration and strain. The frequency of the Si-Si and Ge-Ge modes decrease, as compared to the frequency of pure constituents (Si and Ge respectively). This is caused by the change of the bond lengths and to mass disorder. In addition, for $Si_{1-x}Ge_x$ alloys, one can observe the broadening and asymmetry of the peaks, that are commonly ascribed to the confining effects of phonons induced by the increasing disorder (compared to pure Si or Ge). Another reason for the broadening may come from the non-uniform Ge distribution in the $Si_{1-x}Ge_x$ film (this point will be discussed below). For $Si_{1-x}Ge_x$ alloys, the two effects of mass disorder and bond length, tend to cancel each other and the evolution of the Si-Ge and Ge-Ge frequencies with strain is then lower than the evolution of the Si-Si (~500cm^{-1}) mode.

Moreover, since this frequency is sensitive to both composition and strain of the alloy, the composition should be first determined to evaluate the strain independently of the composition.

In this study, the $Si_{1-x}Ge_x$ compositions were estimated from ToF-SIMS measurements not shown here. Therefore, the exact strain ε value of the $Si_{1-x}Ge_x$ films could be determined by measuring the peak position of the Si-Si mode, according to the following empirical relationship [53]:

$$\omega(x,\varepsilon)_{Si-Si} = 520.5 - 70x + b_{Si}\varepsilon \qquad (Eq.1)$$

where the coefficient b_{Si} is a phenomenological parameter that depends on the elastic constant of the Si and being previously determined by Pezzoli et al [50] at $-730cm^{-1}$. From the measured peaks positions and the Ge concentrations, we were able to deduce the value of the strain in the three $Si_{1-x}Ge_x$ layers. At this scale (a few tens of μm^2), there are significant compressive strains in the three samples with 1.81%, 1.92% and 2.78% measured in the samples A ($Si_{0.7}Ge_{0.3}$), B ($Si_{0.67}Ge_{0.33}$) and C ($Si_{0.5}Ge_{0.5}$) respectively. These values are consistent with the values deduced from elastic theory of fully strained $Si_{1-x}Ge_x$ layers with x=0.3, 0.33 and 0.5 Ge concentrations respectively [55]. They also confirm the absence of plastic relaxation in agreement with AFM observations.

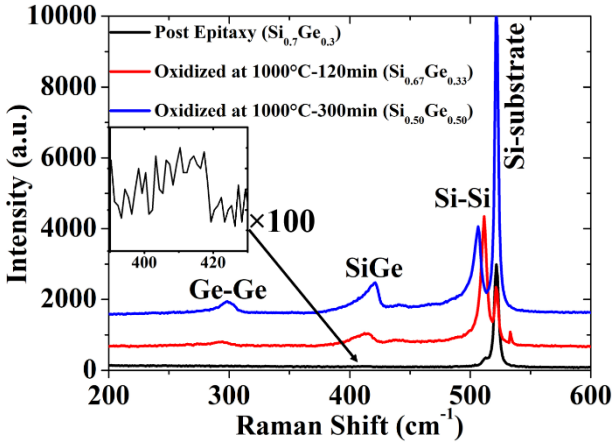

Figure 5: Evolution of the Raman spectra of the three $Si_{1-x}Ge_x$ layers as a function of the oxidation time: Sample A (black line), Sample B (red line) and sample C (blue line). The insert corresponds to a zoom (×100) of the $Si_{1-x}Ge_x$ mode in sample A.

In order to get more local information, strain was quantified locally using GPA on HRTEM images [56]. Cross-section low magnification TEM images of the three samples A, B and C are given in Figures 6. For the three samples, a continuous layer is observed, even if the thickness becomes inhomogeneous for sample C (Figure 6d). The images also confirm the absence of dislocations in the three $Si_{1-x}Ge_x$ films (Figure 6a, 6b and 6c) even if a rotation of the crystallographic planes is observed in sample C (Figure 6e).

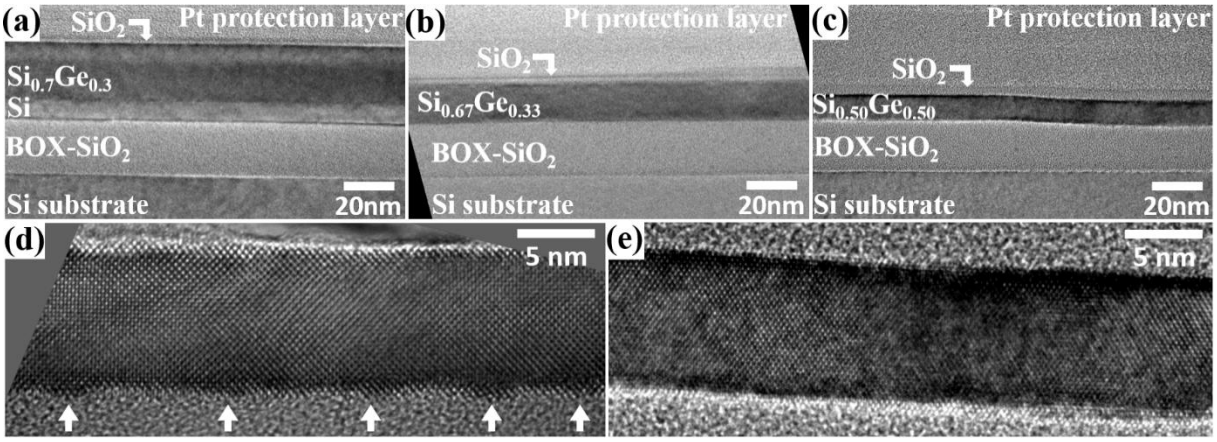

Figure 6: TEM cross-section images (along the [110] crystallographic axis) of the samples A (initial structure) (a), B (oxidized during 120min) (b) and C (oxidized during 300min) (c) where the stacking layers are well visible: Si substrate/20nm BOX/8nm SOI/ $Si_{1-x}Ge_x$ layer and top SiO_2 layer for samples B and C. HRTEM of sample C: (d) arrows indicate the protrusions; (e) small rotation of the crystallographic planes

Figure 7 and 8 give typical GPA strain analyses of the samples A and C respectively together with the corresponding HRTEM images (Figure 7a and 8a). The results for sample B are given in supplementary material S1. The strain profiles are integrated on the images along the in-plane ε_{xx} (Figures 7d and 8d) and the out-of-plane directions ε_{yy} (Figures 7e and 8e). Integration of the deformation along the in-plane x axis (direction parallel to the sample surface) and out-of-plane y axis (perpendicular to the sample surface) are also plotted at the bottom of the figures. The reference chosen for the GPA analyses is the silicon substrate. We can notice that the GPA profiles of the Si substrate are flat and roughly equal to zero along the cross-section of the three samples (supplementary material S2). About ten GPA measurements were performed on each sample to get a true average of the strain.

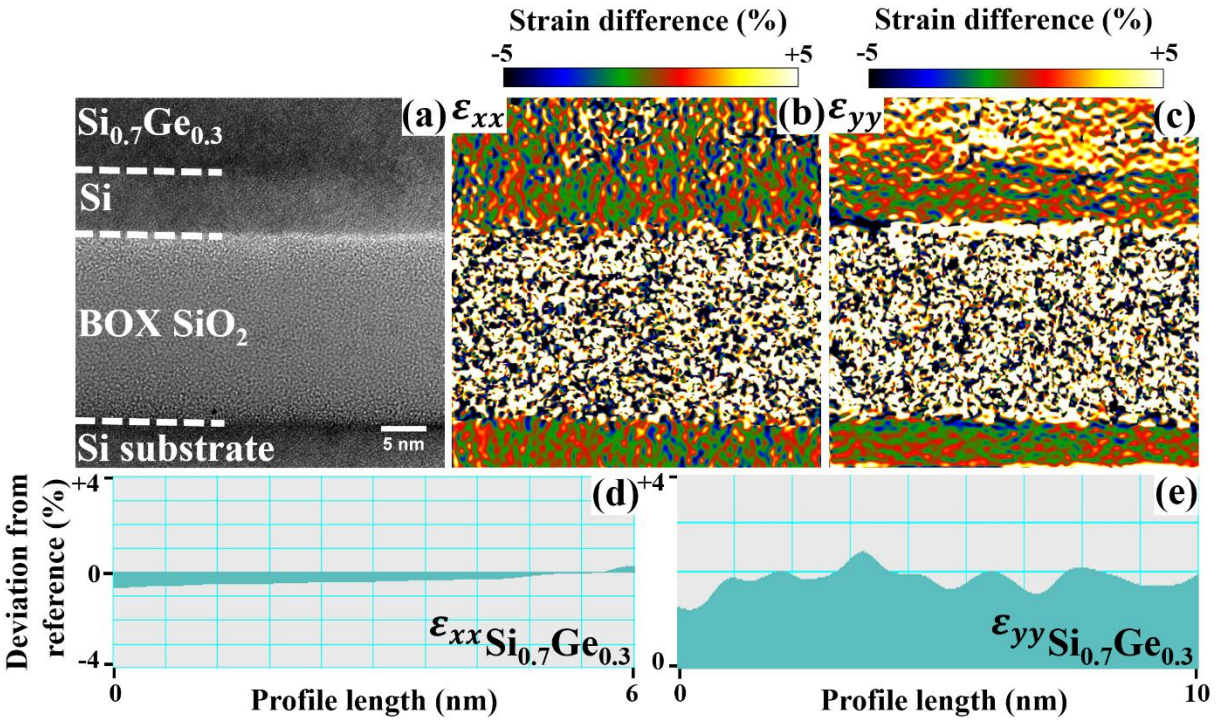

Figure 7: HRTEM cross-sectional image of sample A (a) and GPA of the corresponding image along the x axis ε_{xx} (b) and y axis ε_{yy} (c). (d) and (e) images correspond to the lines profiles of SiGe layer along the x and y axis from GPA images (b) and (c) respectively.

For sample A, there is no variation of the deformation in the x direction, between the silicon substrate, the SOI and the $Si_{0.7}Ge_{0.3}$ layer. This is clearly highlighted by the color code, representative of the deformation, which is the same for the three components: silicon substrate, SOI and $Si_{0.7}Ge_{0.3}$ layer (Figure 7b). These observations indicate that in this direction, the $Si_{0.7}Ge_{0.3}$ layer has the same lattice parameter than bulk Si, without any deformation. In the perpendicular direction, the situation is quite different and the deformation along the out-of-plane y axis in the sample A is well revealed by the different color code of the integrated strain between silicon substrate and $Si_{0.7}Ge_{0.3}$ layer (Figure 7c). One can notice a large increase of about 2% of the lattice parameter of the $Si_{0.7}Ge_{0.3}$ layer as compared to the one of Si in this direction (Figure 7e) which corresponds to the tetragonal distortion of the lattice parameter along the y axis, due to the Poisson's ratio (following Hooke's law). The tetragonal distortion measured all along the sample is homogeneous.

A similar situation is observed for sample B (for details see supplementary material S1): no strain is measured along x and about 2% tetragonal distortion along y. The strain is also homogeneous along the sample surface. One can remark that it is not possible to differentiate the strain between $Si_{0.7}Ge_{0.3}$ and $Si_{0.67}Ge_{0.33}$ due to the precision in the range of 0,1% of the GPA measurements.

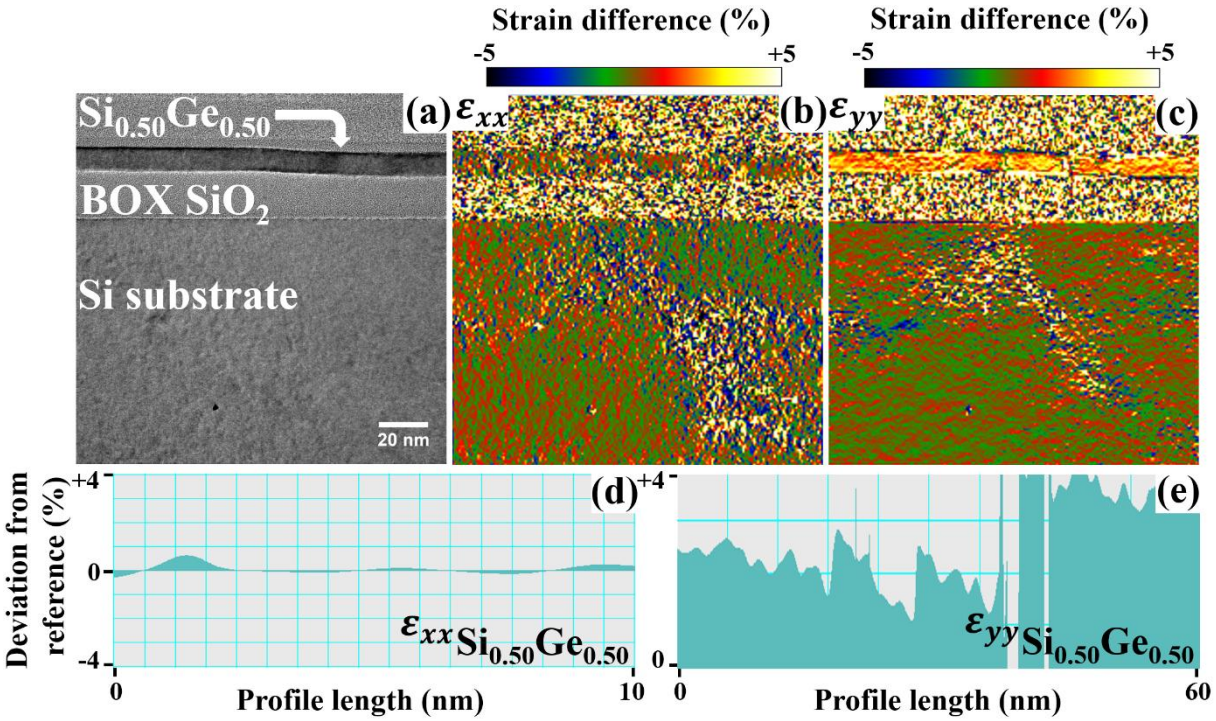

Figure 8: HRTEM cross-sectional image of sample C (a) and GPA of the corresponding image along the x axis ε_{xx} (b) and y axis ε_{yy} (c). (d) and (e) images correspond to the lines profiles of SiGe layer along the x and y axis from GPA images (b) and (c) respectively.

A clearly different situation occurs for sample C. While in the x direction the $Si_{0.50}Ge_{0.50}$ lattice parameter seems constant along the interface and almost the same as the substrate (Figure 8b, 8d), in the perpendicular direction y, the strain is clearly inhomogeneous, as can be seen on both the GPA color code image and the lattice parameter integrated profile (Figure 8c and 8e). The perpendicular strain measured is about 4% in various places (which corresponds well to the tetragonal distortion expected for $Si_{0.50}Ge_{0.50}$), but it can abruptly decrease to around 1% in specific areas. This strain relaxation is accompanied by small protrusions and rotation of the crystallographic planes. The HRTEM images recorded on these areas did not reveal any visible extended defect, even if the corrugation causes a rotation of the crystallographic planes and their local disappearance (Figure 6d). Such rotation hampers the quantitative measurement of strain (in particular ε_{xx}) in these areas which would have required GPA on large integration windows. Nevertheless, much lower integration windows were used and GPA evidence abrupt changes of ε_{yy} which are representative of the strain relaxation in these areas.

In summary, both the Raman and GPA results evidence homogeneous, continuous and fully strained $Si_{1-x}Ge_x$ layers for x=0.3 and x=0.33. The strain measured is in good agreement with the expected tetragonal distortion commonly observed in epitaxial layers. After longer condensation, for $Si_{0.50}Ge_{0.50}$, the situation becomes very different with the onset of strong strain inhomogeneities that can be seen locally. These strain inhomogeneities are accompanied by the undulation and the local thickening (swelling) of the layer, which remains free of extended defect since no defect could be visualized on SEM, AFM and HRTEM cross-section images. The GPA results are in good agreement with the Raman data (Table 1) for samples A and B and both evidence fulky strained layers. For sample C, the situation is more complex since the layer has an inhomogeneous distribution of strain which is

not clearly identified on the Raman spectra. Raman spectra that are averaged over large areas (some μm^2), show that the layer is overall strained. However, when looking in more detail to the strain by GPA, it can be seen that the layer is partly relaxed in several positions. This partial relaxation is accompanied by the undulation of the layer, the rotation of its crystallographic planes and its swelling and thickening.

Table 1 : Out-of-plane strain values estimated from Raman spectroscopy and GPA analysis of the three SiGe layers : $Si_{0.7}Ge_{0.3}$ (sample A), $Si_{0.67}Ge_{0.33}$ (sample B) and $Si_{0.50}Ge_{0.50}$ (sample C).

Samples	**Strain values from Raman spectroscopy (%)**	**Out-of-plane strain values from GPA analysis (%)**
A ($Si_{0.70}Ge_{0.30}$)	1.81	1.90 ± 0.1
B ($Si_{0.67}Ge_{0.33}$)	1.92	2.02 ± 0.05
C ($Si_{0.50}Ge_{0.50}$)	2.78	from 1 to 4 with a large uncertainty

This local relaxation is a very new mechanism which is based on an easy diffusion and redistribution of $Si_{0.50}Ge_{0.50}$ matter along the $Si_{0.50}Ge_{0.50}/SiO_2$ interface accompanied by the undulation (or corrugation) of the layer. Such mechanism would correspond to the relaxation of a free membrane without any interaction with the surrounding matrix, which was not a priori the situation of $Si_{0.50}Ge_{0.50}$ in SiO_2 matrix.

All the data suggest that this phenomenon can be regarded as the first signs of elastic relaxation at the origin of the buckling mechanism, already reported during high temperature annealing of compressively strained $Si_{1-x}Ge_x$ films on a viscous substrate [39, 41, 44, 45]. This mechanism has been commonly related to the low viscosity of the surrounding oxide, which in our conditions, has a glass transition temperature around 965°C. At this temperature, the thermal oxide starts to flow with a temperature-dependent dynamics [57, 58] described by an Arrhenius behavior (equivalent to viscous glass dynamics). When a strained $Si_{1-x}Ge_x$ layer is attached to this viscous SiO_2 layer, it can relax part of its strain by generating wavy morphologies (or ripples). We suggest that the thickening and undulations/ rotation of the crystallographic planes observed in figure 8a for the sample C oxidized at 1000°C during 300min could be considered as the onset of the morphological evolution of the SiGe film, possibly leading in subsequent step to the layer buckling (see supplementary material S3). In our experimental conditions, the strain relaxation takes place throughthe redistribution of $Si_{1-x}Ge_x$ in SiO_2 which is facilitated by the viscous flow of the oxide layer [59]. While techniques exist to reach elastic strain relaxation on small selected areas [60], being able to achieve th is relaxation on a substrate with macroscopic lateral dimensions would be unvaluable. Experiments are under progress to quantitatively determine the strain evolution and distribution in the layer, overall by XRD and locally by GPA, during the morphological evolution of the layer (undulation / buckling phenomenon). An extensive study of the buckling mechanism will be presented elsewhere.

Conclusion

We have shown that the newly developed dry-oxidation process with ultra-low oxygen partial pressure can produce continuous, dislocation free and highly strained Ge rich $Si_{1-x}Ge_x$ layers as testified by Raman analyses and AFM and TEM observations. Local quantitative measurements of strain by HRTEM and GPA evidence a new relaxation mechanism based on an easy redistribution of $Si_{1-x}Ge_x$ in the surrounding SiO_2 layer. This mechanism which occurs during the high temperature oxidation (1000°C) of $Si_{0.7}Ge_{0.3}$ film for 300min, is the result of the viscous flow of SiO_2 at this temperature, which is higher than its glass transition temperature. The relaxation is accompanied by a local swelling and an undulation of the $Si_{1-x}Ge_x$ layer well visible on TEM cross-section images. The control of the buckling amplitude and location has not been investigated so far, but it clearly marks a new way forward to expand the use of Ge rich layer well over the standard critical thickness of relaxation and to develop new device applications employing the buckled and relaxed state of Ge rich $Si_{1-x}Ge_x$ layers based on the dynamic flow of SiO_2. The generic mechanism described here could be extended to many other strained films on viscous substrates.

Acknowledgments

The authors would like to thank NANO2022 for the financial support, CP2M for Microscopy facilities and NANOTECMAT for the nanotechnological equipments and facilities. We also thank Denis ROCHON for Raman characterization.

Corresponding Author

Isabelle.berbezier@im2np.fr

References

[1] Y. H. Xie, Don Monroe, E. A. Fitzgerald, P. J. Silverman, F. A. Thiel, and G. P. Watson, Very high mobility two-dimensional hole gas in Si/GexSi1−x/Ge structures grown by molecular beam epitaxy. Appl. Phys. Lett. 1993, 63, 2263–2264

[2] M. V. Fischetti, S. E. Laux, Band structure, deformation potentials, and carrier mobility in strained Si, Ge, and $Si_{1-x}Ge_x$ alloys. Journal of Applied Physics 1996, 80, 2234

[3] C. M. Engelhardt, D. Többen, M. Aschauer, F. Schäffler, G. Abstreiter, E. Gornik, High mobility 2-D hole gases in strained Ge channels on Si substrates studied by magnetotransport and cyclotron resonance. Solid State Electron 1994, 37, 949–952

[4] K. Ismail, B. S. Meyerson, and P. J. Wang, High electron mobility in modulation- doped Si/SiGe. Appl. Phys. Lett. 1991, 58, 2117

[5] F. Schaffler, D. Tobben, H-J. Herzog, G. Abstreiter and B. Hollander, High-electron-mobility Si/SiGe heterostructures: influence of the relaxed SiGe buffer layer. Semiconductor Science and Technology 1992, 7, 260

[6] S. Verdonckt-Vandebroek, E. F. Crabbe, B. S. Meyerson, D. L. Harame, P. J. Restle, J. M. C. Stork, J. B. Johnson, SiGe-channel heterojunction p-MOSFET's. IEEE Transactions on Electron Devices 1994, 41, 90-101

[7] Y. Sun, S. E. Thompson, and T. Nishida, Physics of strain effects in semiconductors and metal-oxide-semiconductor field-effect transistors. Journal of Applied Physics 2007, 101, 104503

[8] R. Oberhuber, G. Zandler, and P. Vogl, Subband structure and mobility of two-dimensional holes in strained Si/SiGe MOSFET’s. Phys. Rev. B 1998, 58, 9941

[9] T. Ghani, M. Armstrong, C. Auth, M. Bost, P. Charvat, G. Glass, T. Hoffmann, K. Johnson, C. Kenyon, J. Klaus, B. McIntyre, K. Mistry, A. Murthy, J. Sandford, M. Silberstein, S. Sivakumar, P. Smith, K. Zawadzki, S. Thompson and M. Bohr, A 90nm high volume manufacturing logic technology featuring novel 45nm gate length strained silicon CMOS transistors. IEEE International Electron Devices Meeting 2003, Washington, DC, USA, 2003, 11.6.1-11.6.3

[10] Yi Song, Huajie Zhou, Qiuxia Xu, Jun Luo, Haizhou Yin, Jiang Yan, and Huicai Zhong, Mobility Enhancement Technology for Scaling of CMOS Devices: Overview and Status. Journal of Electronic Materials 2011, 40, 1584

[11] T. A. Langdo, M. T. Currie, Z.-Y. Cheng, J. G. Fiorenza, M. Erdtmann, G. Braithwaite, C. W. Leitz, C. J. Vineis, J. A. Carlin, A. Lochtefeld, M. T. Bulsara, I. Lauer, D. A. Antoniadis, M. Somerville, Strained Si on insulator technology: from materials to devices. Solid State Electronics 2004, 48, 1357-1367

[12] Gianni Taraschi, Arthur J.Pitera, Eugene A. Fitzgerald, Strained Si, SiGe, and Ge on-insulator: review of wafer bonding fabrication techniques. Solid-State Electronics 2004, 48, 1297-1305

[13] Ravi Pillarisetty, Academic and industry research progress in germanium nanodevices. Nature 2011, 479, 324–328

[14] Minjoo L. Lee, and Eugene A. Fitzgerald, Strained Si, SiGe, and Ge channels for high-mobility metal-oxide-semiconductor field-effect transistors. Journal of Applied Physics 2005, 97, 011101

[15] EE Haller, Germanium: From its discovery to SiGe devices. Materials science in semiconductor processing 2006, 9, 408-422

[16] Jacopo Franco, Ben Kaczer, Guido Groeseneken, Reliability of High Mobility SiGe Channel MOSFETs for Future CMOS Applications. Springer Series in Advanced Microelectronics book series, MICROELECTR. 2014, 47

[17] Li Shen, Noel Healy, Colin J. Mitchell, Jordi Soler Penades, Milos Nedeljkovic, Goran Z. Mashanovich, and Anna C. Peacock, Mid-infrared all-optical modulation in low-loss germanium-on-silicon waveguides. Optics Letters 2015, 40, 268-271

[18] Yu-Chi Chang, Vincent Paeder, Lubos Hvozdara, Jean-Michel Hartmann, and Hans Peter Herzig, Low-loss germanium strip waveguides on silicon for the mid-infrared. Optics Letters 2012, 37, 2883-2885

[19] J. M. Ramirez, Q. Liu, V. Vakarin, J. Frigerio, A. Ballabio, X. Le Roux, D. Bouville, L. Vivien, G. Isella, and D. Marris-Morini, Graded SiGe waveguides with broadband low-loss propagation in the mid infrared. Optics Express 2018, 26, 870-877

[20] O. Weber, E. Josse, J. Mazurier, N. Degors, S. Chhun, P. Maury, S. Lagrasta, D. Barge, J.P. Manceau, and M. Haond, 14nm FDSOI upgraded device performance for ultra-low voltage operation. Symposium on VLSI Technology 2015, T168–T169

[21] T. Mizuno, S. Takagi, N. Sugiyama, H. Satake, A. Kurobe and A. Toriumi, Electron and hole mobility enhancement in strained-Si MOSFET's on SiGe-on-insulator substrates fabricated by SIMOX technology. IEEE Electron Device Letters 2000, 21, 230-232

[22] Min Chu, Yongke Sun, Umamaheswari Aghoram, and Scott E. Thompson, Strain: A Solution for Higher Carrier Mobility in Nanoscale MOSFETs. Annual Review of Materials Research 2009, 39, 203-229

[23] T. Tezuka, N. Sugiyama, and S. Takagi, Fabrication of strained Si on an ultrathin SiGe-on-insulator virtual substrate with a high-Ge fraction. Applied Physics Letters 2001, 79, 1798

[24] T. Tezuka, Y. Moriyama, S. Nakaharai, N. Sugiyama, N. Hirashita, E. Toyoda, Y. Miyamura, S. Takagi, Lattice Relaxation and Dislocation Generation/Annihilation in SiGe-On-Insulator Layers During Ge Condensation Process. Thin Solid Films 2006, 508, 251− 255.

[25] C.G. Littlejohns, M. Nedeljkovic, C.F. Mallinson, J.F. Watts, G.Z. Mashanovich, G.T. Reed, F.Y. Gardes, Next Generation Device Grade Silicon-Germanium on Insulator. Sci. Rep. 2015, 5, 8288

[26] R. Berthelon, F. Andrieu, S. Ortolland, R. Nicolas, T. Poiroux, E. Baylac, D. Dutartre, E. Josse, A. Claverie, M. Haond, Characterization and modelling of layout effects in SiGe channel pMOSFETs from 14 nm UTBB FDSOI technology. Solid-State Electronics 2017, 128, 72-79

[27] Erich Kasper and Jinzhong Yu, Silicon-Based Photonics. Jenny Stanford Publishing 2020, 352

[28] R. E. Camacho-Aguilera, Y. Cai, N. Patel, J. T. Bessette, M. Romagnoli, L. C. Kimerling, and J. Michel, An electrically pumped germanium laser. Opt. Express 2012, 20, 11316–11320

[29] B. Troia, J. S. Penades, A. Z. Khokhar, M. Nedeljkovic, C. Alonso-Ramos, V. M. N. Passaro, and G. Z. Mashanovich, Germanium-on-silicon Vernier-effect photonic microcavities for the mid-infrared. Opt. Lett. 2016, 41, 610–613

[30] S. Nakaharai, T. Tezuka, N. Sugiyama, Y. Moriyama, and S. Takagi, Characterization of 7-nm-thick strained Ge-on-insulator layer fabricated by Ge-condensation technique. Applied Physics Letters 2003, 83, 3516

[31] F. K. LeGoues, R. Rosenberg, and B. S. Meyerson, Kinetics and mechanism of oxidation of SiGe: dry versus wet oxidation. Applied Physics Letter 1989, 54, 644

[32] Guangyang Lin, Dongxue Liang, Jiaqi Wang, Chunyu Yu, Cheng Li, Songyan Chen, Wei Huang, Jianyuan Wang and Jianfang Xu, Strain evolution in SiGe-on-insulator fabricated by a modified germanium condensation technique with gradually reduced condensation temperature. Materials Science in Semiconductor Processing 2019, 97, 56-61

[33] B. Vincent, J.-F. Damlencourt, V. Delaye, R. Gassilloud, L. Clavelier, and Y. Morand, Stacking fault generation during relaxation of silicon germanium on insulator layers obtained by the Ge condensation technique. Applied Physics Letters 2007, 90, 074101

[34] L. Souriau, G. Wang, R. Loo, M. Caymax, M. Meuris, M. M. Heyns, and W. Vandervorst, Comprehensive Study of the Fabrication of SGOI Substrates by the Ge Condensation Technique: Oxidation Kinetics and Relaxation Mechanism. ECS Trans. 2009, 25, 363

[35] N. Sugiyama, T. Tezuka, T. Mizuno, M. Suzuki, Y. Ishikawa, N. Shibata, and S. Takagi, Temperature effects on Ge condensation by thermal oxidation of SiGe-on-insulator structures. Journal of Applied Physics 2004, 95, 4007

[36] T. Tezuka, N. Sugiyama, T. Mizuno, M. Suzuki and S. Takagi, A Novel Fabrication Technique of Ultrathin and Relaxed SiGe Buffer Layers with High Ge Fraction for Sub-100

nm Strained Silicon-on-Insulator MOSFETs. Japanese Journal of Applied Physics 2001, 40, 2866

[37] N. A. Davidenko, I. I. Davidenko, V. A. Pavlov, N. G. Chuprina, V. V. Tarasenko and S. L. Studzinsky, Adjustment of diffraction efficiency of polarization holograms in azobenzene polymers films using electric field. Journal of Applied Physics 2017, 122, 013101

[38] Thomas David, Isabelle Berbezier, Jean-Noël Aqua, Marco Abbarchi, Antoine Ronda, Nicolas Pons, Francis Domart, Pascal Costaganna, Gregory Uren, and Luc Favre, New Strategies for Engineering Tensile Strained Si Layers for Novel n-Type MOSFET, ACS Appl. Mater. Interfaces 2021, 13, 1807–1817

[39] K. D. Hobart, F. J. Kub, M. Fatemi, M. E. Twigg, P. E. Thompson, T. S. Kuan, and C. K. Inoki, Compliant substrates: a comparative study of the relaxation mechanisms of strained films bonded to high and low viscosity oxides. Journal of Electronic Materials 2000, 29, 897-900

[40] R. Oberhuber, G. Zandler, and P. Vogl, Subband structure and mobility of two-dimensional holes in strained Si/SiGe MOSFET's. Physical Review B 1998, 58, 9941-9947

[41] R. Huang and Z. Suo, Wrinkling of a compressed elastic film on a viscous layer. Journal of Applied Physics 2002, 91, 1135

[42] J. Liang, R. Huang, H. Yin, J. C. Sturm, K. D. Hobart, and Z. Suo, Relaxation of compressed elastic islands on a viscous layer. Acta Materialia 2002, 50, 2933–2944

[43] H. Yin, R. Huang, K. D. Hobart, Z. Suo, T. S. Kuan, C. K. Inoki, S. R. Shieh, T. S. Duffy, F. J. Kub, and J. C. Sturm, Strain relaxation of SiGe islands on compliant oxide. Journal of Applied Physics 2002, 91, 9716

[44] C.-Y. Yu, C.-J. Lee, C.-Y. Lee, and J.-T. Lee, Buckling characteristics of SiGe layers on viscous oxide. Journal of Applied Physics 2006, 100, 063510

[45] Marika Gunji, Ann F. Marshall, and Paul C. McIntyre, Strain relaxation mechanisms in compressively strained thin SiGe-on-insulator films grown by selective Si oxidation. Journal of Applied Physics 2011, 109, 014324-014324-6

[46] Damien Valenducq, Olivier Gourhant, Elisabeth Blanquet, Fabien Deprat, Francesco Abbate, Veronique Guyader, Denis Rouchon, 2019 Joint International EUROSOI Workshop and International Conference on Ultimate Integration on Silicon (EUROSOI-ULIS)

[47] Thomas David, Abdelmalek Benkouider, Jean-Noël Aqua, Martiane Cabie, Luc Favre, Marco Abbarchi, Meher Naffouti, Antoine Ronda, Kailang Liu, Isabelle Berbezier, Kinetics and Energetics of Ge Condensation in SiGe Oxidation. Journal of Physical Chemistry C 2015, 119, 24606 - 24613

[48] Thomas David, Kailang Liu, Sara Fernandez, Marie-Ingrid Richard, Antoine Ronda, Luc Favre, Marco Abbarchi, Abdelmalek Benkouider, Jean-Noël Aqua, Matthew C. Peters, Peter W. Voorhees, Olivier Thomas, and Isabelle Berbezier, Remarkable Strength Characteristics of Defect-Free SiGe/Si Heterostructures Obtained by Ge Condensation. Journal of Physical Chemistry C 2016, 120, 20333-20340

[49] Thomas Wood, Meher Naffouti, Johann Berthelot, Thomas David, Jean-Benoît Claude, Léo Métayer, Anne Delobbe, Luc Favre, Antoine Ronda, Isabelle Berbezier, Nicolas Bonod, Marco Abbarchi, All-Dielectric Color Filters Using SiGe-Based Mie Resonator Arrays, ACS Photonics 2017, 4, 873–883

[50] Vladimir Poborchii, Mohammed Bouabdellaoui, Noriyuki Uchida, Antoine Ronda, Isabelle Berbezier, Thomas David, Carmen M Ruiz, Mimoun Zazoui, Robert Paria Sena, Marco Abbarchi, Raman microscopy and infrared optical properties of SiGe Mie resonators formed on SiO_2 via Ge condensation and solid state dewetting, Nanotechnology, 2020, 31, 195602

[51] I. Berbezier, M. Aouassa, A. Ronda, L. Favre, M. Bollani, R. Sordan, A. Delobbe, and P. Sudraud, Ordered arrays of Si and Ge nanocrystals via dewetting of pre-patterned thin films, Journal of Applied Physics 2013, 113, 064908

[52] Fabien Rozé, François Pierre, Olivier Gourhant, François Bertin, Elisabeth Blanquet, Denis Rouchon, Crystal quality of SiGe films fabricated by the condensation technique and characterized by medium energy ion scattering. Semiconductor Science and Technology 2019, 34, 065005

[53] G. Capellini, M. De Seta, Y. Busby, M. Pea, F. Evangelisti, G. Nicotra, C. Spinella, M. Nardone, and C. Ferrari, Strain relaxation in high Ge content SiGe layers deposited on Si. Journal of Applied Physics 2010, 107, 063504

[54] F. Pezzoli, E. Bonera, E. Grilli, M. Guzzi, S. Sanguinetti, D. Chrastina, G. Isella, H. von Känel, E. Wintersberger, J. Stangl, and G. Bauer, Raman spectroscopy determination of composition and strain in Si1−xGex/Si heterostructures. Materials Science in Semiconductor Processing 2008, 11, 279-284

[55] T. Tezuka, N. Hirashita, Y. Moriyama, S. Nakaharai, N. Sugiyama, and S. Takagi, Strain analysis in ultrathin SiGe-on-insulator layers formed from strained Si-on-insulator substrates by Ge-condensation process. Applied Physics Letters 2007, 90, 181918

[56] E. Snoeck, B. Warot, H. Ardhuin, A. Rocher, M.J. Casanove, R. Kilaas, M.J. Hÿtch, Quantitative analysis of strain field in thin films from HRTEM micrographs. Thin Solid Films 1998, 319, 157− 162

[57] L. Adami, M. Cerdonio, F. F. Ricci, and G. L. Romani, A superconducting strain transducer. Applied Physics Letters 1977, 30, 240

[58] Robert H. Doremus, Viscosity of silica. Journal of Applied Physics 2002, 92, 7619

[59] J. Liang, R. Huang, H. Yin, J. C. Sturm, K. D. Hobart, and Z. Suo, Relaxation of compressed elastic islands on a viscous layer. Acta Materialia 2002, 50, 2933–2944

[60] Fabio Isa, Marco Salvalaglio, Yadira Arroyo Rojas Dasilva, Mojmír Meduňa, Michael Barget, Arik Jung, Thomas Kreiliger, Giovanni Isella, Rolf Erni, Fabio Pezzoli, Emiliano Bonera, Philippe Niedermann, Pierangelo Gröning, Francesco Montalenti, Hans von Känel,

Highly Mismatched, Dislocation-Free SiGe/Si Heterostructures, Adv. Materials, 28, 884 (2016)

Supporting information for:

Local defect-free elastic strain relaxation of $Si_{1-x}Ge_x$ embedded into SiO_2

Elie Assaf [1], Isabelle Berbezier[1], Mohamed Bouabdellaoui[1], Marco Abbarchi[1], Antoine Ronda[1], Damien Valenducq[2], Fabien Deprat[2], Olivier Gourhant[2], Andreas Campos[3], Luc Favre[1]

[1]*CNRS, IM2NP, Aix-Marseille University, Faculté des Sciences de Saint-Jérôme, case 142, 13397 Marseille, France*

[2]*Digital Front End Manufacturing & Technology STMicroelectronics Crolles, France*

[3]*CP2M, Service 221, Campus Scientifique de Saint Jérôme, 13397 Marseille cedex 20*

E-mail: elie.assaf@im2np.fr

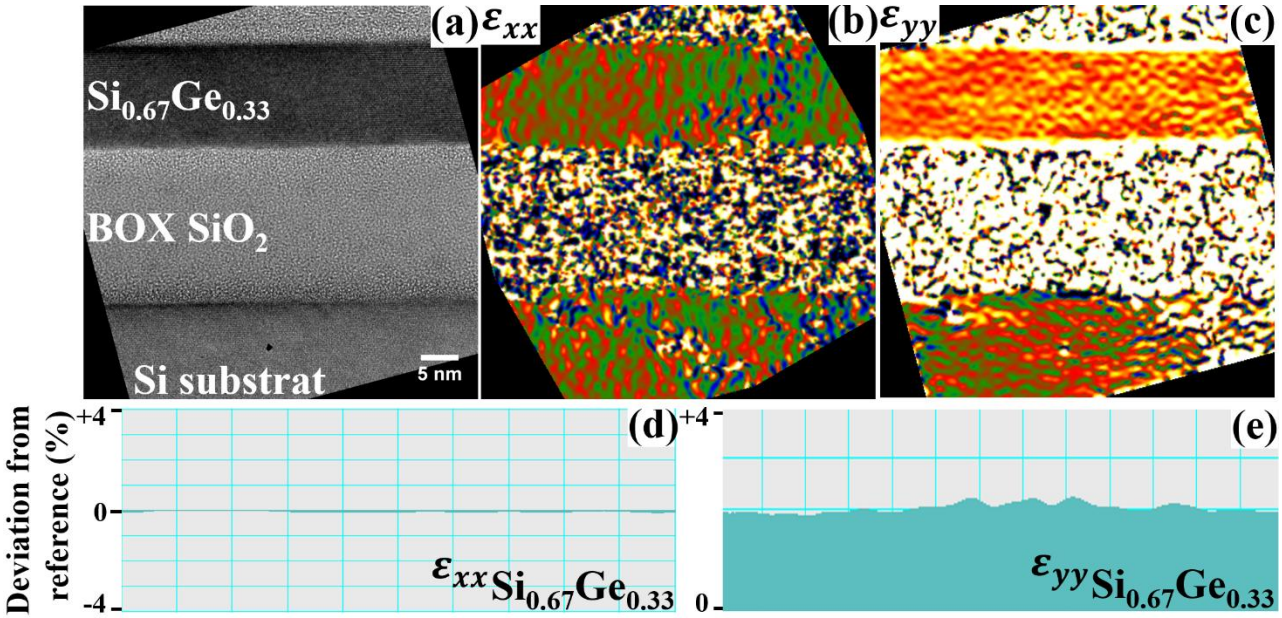

Figure S1: HRTEM cross-sectional image of sample B (a) and GPA of the corresponding image along the x axis (b) and y axis (c). (d) and (e) images correspond to the lines profiles of SiGe layer along the x and y axis from GPA images (b) and (c) respectively.

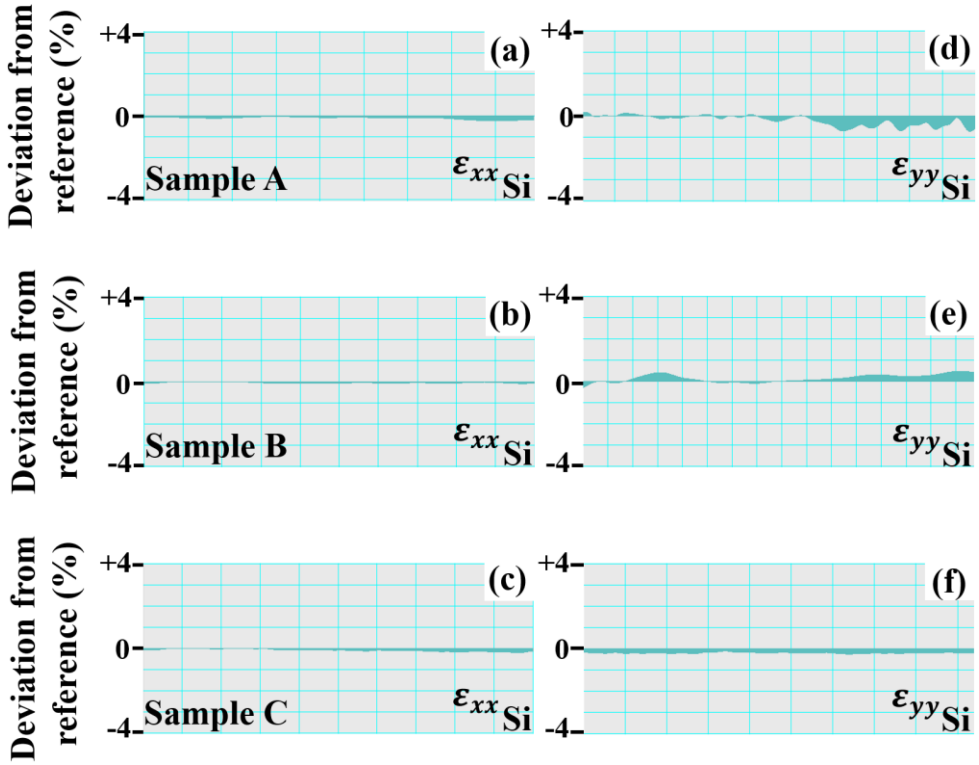

Figure S2: (a), (b) and (c) correspond to the lines profiles of silicon substrate of sample A, B and C along the x axis respectively. (d), (e) and (f) correspond to the lines profiles of silicon substrate of sample A, B and C along the y axis respectively.

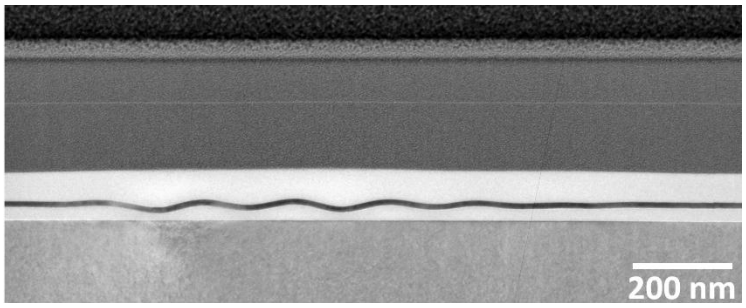

Figure S3: TEM cross-section image of a $Si_{0.50}Ge_{0.50}$ sample where the buckling of the layer is clearly visible.